Density functional with full exact exchange, balanced nonlocality of correlation, and constraint satisfaction

John P. Perdew

Department of Physics, Tulane University, New Orleans, Louisiana 70118, USA

Viktor N. Staroverov

Department of Chemistry, The University of Western Ontario, London, Ontario N6A 5B7, Canada

Jianmin Tao

Theoretical Division and CNLS, Los Alamos National Laboratory, Los Alamos, New Mexico 87545, USA

Gustavo E. Scuseria

Department of Chemistry, Rice University, Houston, Texas 77005, USA
(Dated: October 10, 2008)

We construct a nonlocal density functional approximation with full exact exchange, while preserving the constraint-satisfaction approach and justified error cancellations of simpler semilocal functionals. This is achieved by interpolating between different approximations suitable for two extreme regions of the electron density. In a "normal" region, the exact exchange-correlation hole density around an electron is semilocal because its spatial range is reduced by correlation and because it integrates over a narrow range to -1. These regions are well described by popular semilocal approximations (many of which have been constructed nonempirically), because of proper accuracy for a slowly-varying density or because of error cancellation between exchange and correlation. "Abnormal" regions, where nonlocality is unveiled, include those in which exchange can dominate correlation (one-electron, nonuniform high-density, and rapidly-varying limits), and those open subsystems of fluctuating electron number over which the exact exchange-correlation hole integrates to a value greater than -1. Regions between these extremes are described by a hybrid functional mixing exact and semilocal exchange energy densities locally, i.e., with a mixing fraction that is a function of position $\mathbf{r}$ and a functional of the density. Because our mixing fraction tends to 1 in the high-density limit, we employ full exact exchange according to the rigorous definition of the exchange component of any exchange-correlation energy functional. Use of full exact exchange permits the satisfaction of many exact constraints, but the nonlocality of exchange also requires balanced nonlocality of correlation. We find that this nonlocality can demand at least five empirical parameters, corresponding roughly to the four kinds of abnormal regions. Our local hybrid functional is perhaps the first accurate fourth-rung density functional or hyper-generalized gradient approximation, with full exact exchange, that is size-consistent in the way that simpler functionals are. It satisfies other known exact constraints, including exactness for all one-electron densities, and provides an excellent fit to the 223 molecular enthalpies of formation of the G3/99 set and the 42 reaction barrier heights of the BH42/03 set, improving both (but especially the latter) over most semilocal functionals and global hybrids. Exact constraints, physical insights, and paradigm examples hopefully suppress "overfitting".

PACS numbers: 31.15.ej, 31.10.+z, 71.15.Mb

I. INTRODUCTION

Kohn–Sham density functional theory [1, 2] is a computationally efficient and often usefully accurate approach to electronic structure calculation in condensed matter physics and quantum chemistry. In this theory, the ground-state electron density and total energy E are found by self-consistent solution of a one-electron Schrödinger equation. Only the exchange-correlation (xc) energy as a functional of the density needs to be approximated in practice. This energy can always be written as

$$E_{\mathrm{xc}}[n_\uparrow, n_\downarrow] = \int d^3r\, n(\mathbf{r})\epsilon_{\mathrm{xc}}([n_\uparrow, n_\downarrow]; \mathbf{r}). \quad (1)$$

In this equation, the energy density is the product of the electron density $n(\mathbf{r}) = n_\uparrow(\mathbf{r}) + n_\downarrow(\mathbf{r})$ (the sum of the spin densities) and the position-dependent exchange-correlation energy per electron $\epsilon_{\mathrm{xc}}([n_\uparrow, n_\downarrow]; \mathbf{r})$.

Local or semilocal approximations for $\epsilon_{\mathrm{xc}}([n_\uparrow, n_\downarrow]; \mathbf{r})$, as defined below, are computationally fast and conceptually simple, and can be constructed without empiricism. They work best for sp-block atoms and their molecules and solids around equilibrium. In real systems, full nonlocality is most needed to correct the so-called self-interaction errors [3], which can be most severe in certain stretched-bond situations that arise in transition states for chemical reactions and in the dissociation limit (and also effectively in the d- and f-block systems) [4, 5, 6, 7, 8, 9, 10, 11]. In this paper, we follow

a conservative approach to full nonlocality: We identify those "normal" regions of space in which semilocality is justified, and those "abnormal" ones in which it is not, and then introduce full nonlocality only to the extent that a region is abnormal. The density functional that we construct here shows promising early results, but, whether or not that promise is ultimately fulfilled, the underlying insights could have lasting value.

In popular approximations, $\epsilon_{\mathrm{xc}}([n_\uparrow, n_\downarrow]; \mathbf{r})$ is a function of ingredients at position $\mathbf{r}$, and different selections of ingredients define different rungs of a "Jacob's ladder" [12] of approximations. Accuracy tends to increase up the ladder, while simplicity increases downwards. The first three rungs use semilocal ingredients constructed from the density or orbitals in an infinitesimal neighborhood of $\mathbf{r}$, and have nonempirical [13] (as well as empirical) constructions. The first rung is the local spin density approximation (LSDA) [1, 14, 15], which uses as ingredients $n_\uparrow(\mathbf{r})$ and $n_\downarrow(\mathbf{r})$ and is exact only for a uniform or very slowly-varying electron gas. The second rung is the generalized gradient approximation (GGA), which adds the gradients $\nabla n_\uparrow(\mathbf{r})$ and $\nabla n_\downarrow(\mathbf{r})$, as in the Perdew–Burke–Ernzerhof (PBE) [16] and PBEsol [17] nonempirical constructions. The third rung is the meta-GGA, which adds the positive orbital kinetic energy densities $\tau_\uparrow(\mathbf{r})$ and $\tau_\downarrow(\mathbf{r})$, as in the Tao–Perdew–Staroverov–Scuseria (TPSS) [18, 19, 20] nonempirical construction. Alternatively, the Laplacians $\nabla^2 n_\uparrow(\mathbf{r})$ and $\nabla^2 n_\downarrow(\mathbf{r})$ of the spin densities could be used [21]. Self-consistent calculations with any of the semilocal functionals are relatively easy and efficient, especially if the demand for a single multiplicative effective potential is dropped at the meta-GGA level (as in Refs. 18, 19, 20).

The fourth rung or hyper-GGA [12, 22, 23, 24, 25, 26, 27, 28, 29, 30], with which we will be concerned here, adds a fully nonlocal (i.e., not semilocal) ingredient, the exact-exchange energy per electron $\epsilon_{\mathrm{x}}^{\mathrm{ex}}$. Unlike total energies E, energy densities $n\epsilon_{\mathrm{xc}}$ are non-unique or gauge-dependent. In the conventional gauge,

$$\epsilon_{\mathrm{x}}^{\mathrm{ex(conv)}}(\mathbf{r}) = \frac{1}{2} \int d^3 r' \, \frac{n_{\mathrm{x}}(\mathbf{r}, \mathbf{r}')}{|\mathbf{r}' - \mathbf{r}|}, \qquad (2)$$

where

$$n_{\mathrm{x}}(\mathbf{r}, \mathbf{r}') = -\sum_\sigma \frac{|\rho_\sigma(\mathbf{r}, \mathbf{r}')|^2}{n(\mathbf{r})}, \qquad (3)$$

is the exact-exchange hole density around an electron at $\mathbf{r}$, and

$$\rho_\sigma(\mathbf{r}, \mathbf{r}') = \sum_i f_{i\sigma} \psi_{i\sigma}(\mathbf{r}) \psi_{i\sigma}^*(\mathbf{r}') \qquad (4)$$

is the Kohn–Sham one-particle density matrix for spin σ. The $f_{i\sigma}$ are occupation numbers, typically 0 or 1 except for values in between that can arise when a Kohn–Sham orbital $\psi_{i\sigma}(\mathbf{r})$ is shared with another system [3, 4, 5, 6, 7, 8, 9, 10, 11]. The exact-exchange hole density satisfies the sum rule

$$
\begin{aligned}
\int d^3 r' \, n_{\mathrm{x}}(\mathbf{r}, \mathbf{r}') &= -1 + \sum_\sigma \sum_i f_{i\sigma}(1 - f_{i\sigma}) \frac{|\psi_{i\sigma}(\mathbf{r})|^2}{n(\mathbf{r})} \\
&= -1 + \Delta_{\mathrm{x}}(\mathbf{r}), \qquad (0 \leq \Delta_{\mathrm{x}} \leq 1) \quad (5)
\end{aligned}
$$

and the right-hand side of Eq. (5) reduces to -1 when all occupation numbers are 0 or 1. A rigorous proof of the exchange-only equations (2)–(5) for an open system of fluctuating electron number is given in Ref. 10. There is also a fifth rung (e.g., Ref. 31) which adds all the occupied *and* unoccupied orbitals as ingredients. While the fourth- and fifth-rung functionals can also be implemented fully self-consistently, tests and applications using, say, meta-GGA orbitals (as in the present work) are easier and more efficient and often suffice.

As we ascend the ladder, the additional ingredients can be used to satisfy additional exact constraints on $E_{\mathrm{xc}}[n_\uparrow, n_\downarrow]$ (nonempirical approach [12, 13]), or to fit data better (empirical approach), or both. As we will see here, many additional constraints can be satisfied on the fourth rung, including exactness for all one-electron densities [3, 12, 23] and full exact exchange [12], but for the first time some empiricism becomes unavoidable (although it can be avoided again on the fifth rung [31]).

There are good reasons for these particular choices of ingredients. The local density suffices for a uniform electron gas. The density gradients contribute to second-order gradient expansions [32, 33, 34] for densities that vary slowly over space, and can also satisfy other constraints [16]. The positive orbital kinetic energy density is relevant to exchange [18, 35] and in particular to its fourth-order gradient expansion [18, 36], and can be used to zero out the correlation energy density in one-electron regions [18, 37]. The Kohn–Sham orbitals needed to construct the higher-rung ingredients are themselves fully nonlocal but implicit functionals of the density. (Strictly, the orbitals are density functionals when the optimum effective potential is required to be a function of position $\mathbf{r}$. In practice, ground-state densities and energies are not much affected when this requirement is dropped, as it often is for computational convenience in self-consistent implementations of meta-GGA's.)

The ladder classification is not intended to be exclusive. Range-separated hybrids [9, 38, 39] that use the exact-exchange hole density of Eq. (3) fall slightly above the fourth rung but well below the fifth. Fully nonlocal "two-point" approximations or six-dimensional integrals that are explicit functionals of the density are also possible, and can provide a long-range van der Waals interaction [40] that is still missing from our local hybrid functional, but implicit density functionals with a nonlocal dependence upon the orbitals are probably needed to describe the situation in which electrons are shared between open subsystems [4, 5, 6, 7, 8, 9, 10].

There are two principal reasons why density functionals should be constructed to satisfy known exact constraints. The first is idealistic: Our approximations

should not needlessly violate what we know to be true. The second is practical: Satisfaction of many constraints helps the approximation to work over a wider range of densities. For example, functionals that are constructed only by fitting to molecular data are less accurate for solids than functionals that satisfy solid-state-like constraints such as the uniform gas limit [41], which by itself fully defines the first or LSDA rung of the ladder.

At the second or GGA rung, the constraints are already less constraining. There are several different sets of constraints that can be imposed on this rung, and some are (for this limited form) incompatible with others [16, 17]. Even for a chosen set of constraints, there may be quite different ways in which they can be satisfied [42]. Thus, the nonempirical GGAs are in practice guided by some additional physical postulate. For the PBE GGA, this guiding postulate is the sharp (atomic-like) cutoff of the spurious long-range part of the gradient expansion for the exchange-correlation hole [43]. For the PBEsol GGA for solids, it is restoration of the gradient expansion for the exchange energy over a wide range of slowly- or moderately-varying densities [17].

We close this introduction by summarizing some of the successes and failures of the TPSS meta-GGA, the nonempirical functional on the highest semilocal rung of the ladder. For the standard enthalpies of formation of the 223 molecules of the G3/99 test set [44] (including COF_2), the mean absolute error (MAE) computed self-consistently using the fully uncontracted 6-311++G(3df,3pd) basis set is only 6.5 kcal/mol when TPSS exchange is combined with TPSS correlation. The MAE increases to 30.3 kcal/mol when full exact exchange is combined with TPSS correlation, and to 211.0 kcal/mol for exact exchange and no correlation (i.e., Hartree–Fock). Thus, atoms and molecules at equilibrium, with integer electron numbers, are predominantly normal systems in which the errors of semilocal exchange and semilocal correlation tend to cancel. This does *not* mean that semilocal functionals always predict realistic binding energy curves. In fact, they do so only when the fragments have integer electron numbers. Asymmetric molecules, when described by semilocal functionals, often dissociate to fragments of spurious fractional charge, for which the energy is seriously too low (Ref. 6 and references therein). Even when the fractional charge is real, as in the dissociation of X_2^+, the self-interaction error of semilocal functionals makes the energy seriously too low (Ref. 7, and references therein) at the dissociation limit $X^{+1/2} \cdots X^{+1/2}$, where it ought to be equal to that of $X^0 \cdots X^{+1}$. The combination of stretched bonds and noninteger average (hence fluctuating) electron numbers on the fragments makes for a highly abnormal valence region. A milder version of the same abnormality is found for the moderately stretched bonds in the transition state of a chemical reaction, where semilocal functionals predict reaction barriers that are too low or even negative.

II. LOCAL HYBRID FORM OF THE HYPER-GGA

The earliest hyper-GGAs were the global hybrid functionals [19, 45, 46, 47], for which the simplest form is

$$E_{xc}^{gh} = aE_x^{ex} + (1-a)E_x^{sl} + E_c^{sl}. \tag{6}$$

Here E_x^{sl} and E_c^{sl} are semilocal exchange and correlation functionals, E_x^{ex} is the exact-exchange energy, and a is a universal, position-independent empirical mixing fraction between 0 and 1. While semilocal approximations ($a = 0$) typically overestimate the atomization energies of molecules [19, 48] and underestimate the energy barriers to chemical reactions [49], the use of exact or Hartree–Fock exchange ($a = 1$) makes opposite errors. Fitting Eq. (6) to atomization energies often gives $a \approx 0.2$, while the reaction barrier heights typically require $a \approx 0.5$. For some systems and properties, even $a \approx 0.2$ is too large [50]. The smallness of a indicates that semilocal exchange is more compatible with semilocal correlation than is the exact, fully nonlocal exchange. The global hybrid functionals are perhaps the most popular functionals in modern quantum chemistry. (Screened hybrid functionals [51] are also gaining popularity for solid-state calculations [52, 53]). They often improve upon the semilocal functionals, at the sometimes-acceptable additional cost of a Hartree–Fock calculation, and the improvement can be pushed further by the addition of further empirical parameters [47]. However, they satisfy no exact constraint beyond those satisfied by the underlying semilocal E_x^{sl}.

A natural generalization to Eq. (6) is the local hybrid functional

$$\begin{aligned}
\epsilon_{xc}^{lh}(\mathbf{r}) &= a(\mathbf{r})\epsilon_x^{ex}(\mathbf{r}) + [1 - a(\mathbf{r})]\epsilon_x^{sl}(\mathbf{r}) + \epsilon_c^{sl}(\mathbf{r}) \\
&= \epsilon_x^{ex}(\mathbf{r}) + [1 - a(\mathbf{r})][\epsilon_x^{sl}(\mathbf{r}) - \epsilon_x^{ex}(\mathbf{r})] + \epsilon_c^{sl}(\mathbf{r})
\end{aligned} \tag{7}$$

where $0 \leq a(\mathbf{r}) \leq 1$. Eq. (7) was first proposed in Ref. 22, without a form for $a(\mathbf{r})$. Forms were proposed in Ref. 12 and Ref. 23 (where the term "local hybrid" was coined), but those forms did not achieve high accuracy for equilibrium properties of molecules.

The choice $\epsilon_{xc}^{sl} = \epsilon_{xc}^{TPSS}$ and $a(\mathbf{r}) = 1$ in Eq. (7) satisfies nearly all exact constraints that a hyper-GGA can satisfy, but yields very poor atomization energies of molecules (as shown in Ref. 12, for example) because it misses the delicate and helpful error cancellation between semilocal exchange and semilocal correlation that typically occurs (because the exact xc-hole is deeper and more short-ranged than the exact x-hole) in "normal" regions of space (as defined in section III). From this fact, it is already clear that the known exact constraints do not tell us how much full nonlocality is needed in correlation for compatibility with exact exchange. The imbalance between nonlocal approximate exchange and semilocal approximate correlation may also be responsible for the inaccuracies of the Perdew–Zunger self-interaction correction [3] and of the local hybrid functional of Ref. 23, when applied to atomization energies.

As envisioned in Ref. 12 and discussed below in section IV A, a hyper-GGA has full exact exchange if it satisfies the exact constraint [54] (for any system with a nondegenerate Kohn–Sham noninteracting ground state)

$$\lim_{\lambda \to \infty} \frac{E_{\text{xc}}[n_\lambda]}{E_{\text{x}}^{\text{ex}}[n_\lambda]} = 1 \qquad (8)$$

under uniform density scaling

$$n(\mathbf{r}) \to n_\lambda(\mathbf{r}) = \lambda^3 n(\lambda \mathbf{r}) \qquad (9)$$

to the high-density limit $\lambda \to \infty$. (Note that $n(\mathbf{r})$ and $n_\lambda(\mathbf{r})$ have the same electron number). Such a functional will automatically satisfy all exact constraints on exchange alone. Of several developed hyper-GGAs [24, 25, 26, 27, 28, 29, 55], the only one that seems to have this property is that of Refs. 26, 27, and 55, for which the correlation energy is not exactly size-consistent. Our size-consistent local hybrid has full exact exchange because its mixing fraction $a(\mathbf{r})$ tends rapidly enough to 1 in the high-density limit, while $\epsilon_{\text{x}}^{\text{ex}} \sim \lambda$, $\epsilon_{\text{x}}^{\text{sl}} \sim \lambda$, and $\epsilon_{\text{c}}^{\text{sl}} \sim \lambda^0$ in this limit. Formally, the exchange part of any $E_{\text{xc}}[n]$ is [54]

$$E_{\text{x}}[n] = \lim_{\lambda \to \infty} \frac{E_{\text{xc}}[n_\lambda]}{\lambda}. \qquad (10)$$

Equation (10) is the only non-arbitrary way to define the exchange component of a density functional for the exchange-correlation energy.

Thus, the three terms in the last line of Eq. (7) represent respectively exact exchange, the fully nonlocal part of correlation including "left-right" [56] static or near-degeneracy correlation important in molecules, and the semilocal dynamic correlation. Instead of thinking of $a(\mathbf{r})$ as the fraction of exact exchange mixed locally with semilocal exchange, it is more correct to think of $[1 - a(\mathbf{r})]$ as the fraction of the nonlocal energy difference $[\epsilon_{\text{x}}^{\text{sl}}(\mathbf{r}) - \epsilon_{\text{x}}^{\text{ex}}(\mathbf{r})]$ added to exact exchange plus semilocal correlation. The quantity $[\epsilon_{\text{x}}^{\text{sl}}(\mathbf{r}) - \epsilon_{\text{x}}^{\text{ex}}(\mathbf{r})]$ is the nonlocality error (and arguably often the self-interaction error) of the semilocal $\epsilon_{\text{x}}^{\text{sl}}$. In a normal region ($a \approx 0$), it provides an estimate of the nonlocal part of the correlation energy (such as the static correlation). In an abnormal region, the semilocal functionals often overestimate [10] the nonlocal correction to correlation, and their estimate must be scaled back. Our $a(\mathbf{r})$ is mnemonic for and measures the "abnormality" of a region of space.

We have recently argued [10] that Eq. (7) could be useful not only for molecules and solids near equilibrium, but even for the more challenging problem of stretched bonds between open subsystems with noninteger average electron number. In such subsystems, in the limit of infinite bond stretch, the total energy variation with electron number between adjacent integers is concave downward for exact exchange [10], concave upward for semilocal exchange or exchange-correlation [5], and linear in an exact description [4, 5], justifying the local-hybrid mixing of Eq. (7). To the extent that a functional mimics the exact

linearity, it is said to be "many-electron self-interaction-free" [6, 7, 8]. We have also discussed [10] in a general way how $a(\mathbf{r})$ should be much less than 1 in normal regions where $\epsilon_{\text{xc}}^{\text{sl}}$ can be accurate, but should approach 1 in many abnormal regions where $\epsilon_{\text{xc}}^{\text{sl}}$ cannot be accurate. We shall construct $a(\mathbf{r})$ in sections III and IV. This construction will necessarily be complicated, because we aim to satisfy as many exact constraints as possible. Our construction will explain why the more complicated hyper-GGAs [24, 25, 26, 27] (including ours) require typically four or five empirical parameters to balance the full nonlocality of correlation with that of exchange. (The hyper-GGAs of Refs. 24, 25, 26, 27 have additional empirical parameters in their semilocal parts, while our hyper-GGA does not.)

To satisfy as many constraints as possible, we will take

$$\epsilon_{\text{x}}^{\text{sl}}(\mathbf{r}) = \epsilon_{\text{x}}^{\text{TPSS}}(\mathbf{r}), \qquad \epsilon_{\text{c}}^{\text{sl}}(\mathbf{r}) = \epsilon_{\text{c}}^{\text{TPSS}}(\mathbf{r}). \qquad (11)$$

The TPSS meta-GGA [18, 19, 20] is constructed nonempirically to satisfy those exact constraints that a meta-GGA can, including the constraint $\epsilon_{\text{c}}(\mathbf{r}) = 0$ in one-electron regions.

A complication arises because of the non-uniqueness of the exchange energy density: many different energy densities can integrate to the same energy. In Eq. (7), we want $\epsilon_{\text{x}}^{\text{ex}}(\mathbf{r})$ to be as similar to $\epsilon_{\text{x}}^{\text{sl}}(\mathbf{r})$ as it can be, so we write [57]

$$n(\mathbf{r})\epsilon_{\text{x}}^{\text{ex}}(\mathbf{r}) = n(\mathbf{r})\epsilon_{\text{x}}^{\text{ex(conv)}}(\mathbf{r}) + \nabla \cdot [U(\mathbf{r})\nabla V(\mathbf{r})], \quad (12)$$

where $\epsilon_{\text{x}}^{\text{ex(conv)}}$ is the conventional exact-exchange energy per electron from Eq. (2). The functions $U(\mathbf{r})$ and $V(\mathbf{r})$ are constructed from hyper-GGA ingredients in Ref. 57. The divergence of the vector field $U\nabla V$ in Eq. (12) integrates over $\mathbf{r}$ to zero. The divergence term is largest in regions where the density is dominated by a single orbital shape, such as one-electron and tail regions; omitting it increases the errors of our local hybrid functional quantitatively but not qualitatively. The global hybrids of Eq. (6) are of course invariant under any choice of gauge.

We have argued that the empirical and nonempirical approaches to density functional approximation must flow together at the hyper-GGA level, as they need not on the three lower rungs of the ladder. On this fourth rung, the world is almost turned upside down: Up to a point, building more physics into a hyper-GGA demands more and not fewer empirical parameters. (A similar situation arises in the construction of explicit density functionals for the orbital kinetic energy [21].)

Simple one-parameter local hybrid functionals, satisfying few or no exact constraints beyond those of the lower-rung functionals, have been constructed by Kaupp and collaborators [28, 29]. More complicated functionals with four or five empirical parameters have been developed using all three standard physical approaches to density functional approximation:

(a) Modeling [35, 43] the exchange-correlation hole around an electron, including the static-correlation part

that arises in stretched-bond H_2, leads to Becke's hyper-GGA [24, 25]. Because Becke starts from a system that has an *exact* degeneracy of its Kohn–Sham noninteracting ground state, he is able to avoid some of the symmetry breaking that persists in our and other hyper-GGAs, but at the cost of violating the exact constraint of Eq. (8) for all ground states without such an unusual degeneracy. For any system in which Becke's hyper-GGA and ours predict a non-zero static correlation energy, the ratio of static correlation to exchange energies under uniform density scaling to the high-density limit will remain unchanged for Becke's hyper-GGA while it will tend to zero for ours; the latter behavior is the correct one in the normal case where the static correlation in the unscaled system arises from a near- but not exact degeneracy.

(b) Modeling [45, 46, 58] the adiabatic connection [59] between the Kohn–Sham Slater determinant and the true interacting wave function leads to the hyper-GGA of Yang and collaborators [26, 27], but with a loss of size consistency (in the weak sense in which simpler functionals are size-consistent). Without size consistency, the energy of a subsystem (e.g., an atom or molecule) can depend upon the presence of another (e.g., a metal surface) even in the limit of infinite separation and even without charge transfer between the subsystems. Size consistency can be preserved by using energy densities, as here and in Refs. 24, 25. It is lost when total energies are used nonlinearly.

(c) Satisfaction [16, 18, 60] of exact constraints on $E_{xc}[n_\uparrow, n_\downarrow]$ leads to our local hybrid.

Hyper-GGAs have also been constructed by fitting a large number of empirical parameters to chemical data sets (e.g., Refs. 47 and 61), while satisfying relatively few exact constraints. In particular, the M06-HF hyper-GGA of Zhao and Truhlar [61] is claimed to have "full Hartree-Fock exchange", but like Becke's hyper-GGA [24, 25] it contains in addition other terms (semi-local ones in this case) which improperly scale like exchange in the high-density limit. Plots [47] of the enhancement factors of the semi-local parts of the parent functional M05-2X display wiggles and other anomalous behaviors suggesting more parameters and fewer constraints than are needed.

Our hyper-GGA work here is distinguished from that of others in two principal ways: (i) We aim to understand fully and build in the error cancellation [10] between semilocal exchange and semilocal correlation that is responsible for much of the success of simpler functionals. (ii) We aim to satisfy nearly all the known exact constraints that a hyper-GGA can, in order to test and apply this exact knowledge and to make our functional useful even in systems and situations very different from those where we have fitted or tested it. One example of such a system is jellium uniaxially compressed toward the true two-dimensional limit [62]. For this challenging problem of dimensional cross-over, our local hybrid functional is significantly better than LSDA, PBE GGA, or TPSS meta-GGA, although not as good as the fifth-rung functional described in Ref. 31.

III. WHY THE EXACT EXCHANGE-CORRELATION HOLE IS SEMILOCAL IN NORMAL REGIONS

The exact exchange-correlation energy can be written [59, 63] in the form of Eq. (1), where in the conventional gauge

$$\epsilon_{xc}^{ex(conv)}(\mathbf{r}) = \frac{1}{2} \int d^3 r' \int_0^1 d\alpha \, \frac{n_{xc}^{ex,\alpha}(\mathbf{r}, \mathbf{r}')}{|\mathbf{r}' - \mathbf{r}|}$$
$$= \frac{1}{2} \int_0^\infty du \, 4\pi u \bar{n}_{xc}^{ex}(\mathbf{r}, u). \qquad (13)$$

Here $\bar{n}_{xc}^{ex}(\mathbf{r}, u)$ is the spherical average over the direction of $\mathbf{u} = \mathbf{r}' - \mathbf{r}$ of the average over coupling constant α of $n_{xc}^{ex,\alpha}(\mathbf{r}, \mathbf{r}')$, where the density is held fixed as α varies from 0 to 1 in the Coulomb interaction $\alpha/|\mathbf{r}' - \mathbf{r}|$, and $n_{xc}^{ex,\alpha=0}(\mathbf{r}, \mathbf{r}') = n_x^{ex}(\mathbf{r}, \mathbf{r}')$. The exact xc-hole obeys the sum rule

$$\int_0^\infty du \, 4\pi u^2 \bar{n}_{xc}^{ex}(\mathbf{r}, u) = -1 + \Delta_{xc}(\mathbf{r}), \qquad (0 \le \Delta_{xc} \le 1),$$
$$(14)$$

where Δ_{xc} vanishes if the integrated electron number in the system does not fluctuate [5, 10]. In the absence of exact degeneracy of the Kohn–Sham noninteracting system, the $\alpha = 0$ limit of $-1 + \Delta_{xc}$ is shown on the extreme right-hand side of Eq. (5). For the slowly-varying densities on which the semilocal approximations are based, $\Delta_{xc} = \Delta_x = 0$. For the LSDA, $\bar{n}_{xc}^{LSDA}(\mathbf{r}, u) = \bar{n}_{xc}^{unif}(n_\uparrow(\mathbf{r}), n_\downarrow(\mathbf{r}); u)$; for the other semilocal approximations, the hole can be either modeled from the start [35, 43] or reverse-engineered [64, 65].

Gunnarsson and Lundqvist [63] gave an argument for the success of LSDA and hence of other semilocal approximations: These approximations satisfy the correct sum rule (when $\Delta_{xc} = 0$), which is by Eq. (14) the second moment of the hole density. Then the energy per electron, which is by Eq. (13) the first moment of the hole density, should not be too wrong. This argument was expanded by Burke, Perdew and Ernzerhof [66] who argued that the small-u behavior (through order u^2) of $\bar{n}_x^{ex}(\mathbf{r}, u)$ is determined exactly by semilocal information, and the small-u behavior (through order $|u|$) of $\bar{n}_c^{ex}(\mathbf{r}, u)$ is often determined approximately by local information. They also argued that the system average arising in Eq. (1) unweights regions of space in which the small-u behavior of $\bar{n}_{xc}^{ex}(\mathbf{r}, u)$ is not so well described by semilocal information. This system average also eliminates the differences between different energy-density gauges.

This argument is easily extended to explain why the semilocal approximations usually work better for exchange and correlation together than for either separately: Correlation makes $\bar{n}_{xc}^{ex}(\mathbf{r}, u)$ deeper at small u, and more short-ranged, than $\bar{n}_x^{ex}(\mathbf{r}, u)$. A deep, narrow xc-hole density, integrating to -1 and having a semilocal small-u behavior, is semilocal.

We define a normal region of space [10] as one in which $\bar{n}_{xc}^{ex}(\mathbf{r}, u)$ is modeled reasonably well by a semilocal ap-

proximation, at least after the system average over that region. The electron density in a normal region is either reasonably slowly-varying, or reasonably low and many-electron-like, or both. Only at sufficiently low and many-electron-like density is correlation comparable in strength to exchange, making possible a useful error cancellation between them. In a normal region, we want $a(\mathbf{r}) \approx 0$ in Eq. (7) to take advantage of the proper accuracy of semilocal approximations (for a slowly-varying density) or of the error cancellation between semilocal exchange and semilocal correlation.

Semilocal information $(n, \nabla n, \tau)$ is enough to tell us whether a density is slowly-varying, low, or many-electron-like. We shall take advantage of this in section IV A. The fully nonlocal information in $\epsilon_{\mathrm{x}}^{\mathrm{ex}}$ of Eqs. (2) and (12) can tell us how big Δ_{x} is. Exact or near degeneracies can make Δ_{xc} small or zero even when Δ_{x} is not small or zero (as in infinitely-stretched spin-unpolarized H_2), but in those cases spin-symmetry breaking can still rescue the semilocal approximations by restoring the correct small-u behavior [67]. We shall make use of this in section IV B.

In a normal region, we will take $a(\mathbf{r})$ in Eq. (7) to be small or zero. Conversely, an abnormal region is one in which we have no clear reason to keep $a(\mathbf{r})$ small, and can let $a(\mathbf{r})$ approach 1.

By the way, we can write the spherically-averaged exchange-correlation hole that yields our local hybrid functional of Eq. (7) as

$$
\begin{aligned}
\bar{n}_{\mathrm{xc}}^{\mathrm{lh}}(\mathbf{r}, u) \;=\; & \bar{n}_{\mathrm{x}}^{\mathrm{ex}}(\mathbf{r}, u) + [1 - a(\mathbf{r})][\bar{n}_{\mathrm{x}}^{\mathrm{TPSS}}(\mathbf{r}, u) - \bar{n}_{\mathrm{x}}^{\mathrm{ex}}(\mathbf{r}, u)] \\
& + \bar{n}_{\mathrm{c}}^{\mathrm{TPSS}}(\mathbf{r}, u).
\end{aligned}
\tag{15}
$$

The TPSS hole is known [65]. Note that the middle term on the right of Eq. (15) is purely long range in u [and of infinite range when $\bar{n}_{\mathrm{x}}^{\mathrm{ex}}(\mathbf{r}, u)$ is], confirming our interpretation of this term as the nonlocal or static correlation.

IV. MIXING EXACT EXCHANGE IN ABNORMAL REGIONS WHERE THE HOLE IS FULLY NONLOCAL

Our hyper-GGA is the local hybrid functional of Eqs. (7), (8), and (11). The motivation for this form was presented in section II, and the idea behind the local exact-exchange mixing fraction $a(\mathbf{r})$ was explained in section III and Ref. 10: We want to satisfy essentially all possible exact constraints on $E_{\mathrm{xc}}[n_\uparrow, n_\downarrow]$, including Eq. (8) which guarantees that our hyper-GGA has full exact exchange, while preserving the proper accuracy or the error cancellation between semilocal exchange and semilocal correlation that occurs in normal regions

Thus we want $a(\mathbf{r}) \approx 0$ in a normal region, and $a(\mathbf{r}) \approx 1$ in strongly abnormal regions. An abnormal region is one in which the density is (i) one-electron-like, rapidly-varying over space, or nonuniform and high, or (ii) strongly fluctuating in electron number. We will define an $a_1(\mathbf{r})$ and an $a_2(\mathbf{r})$ in subsections IV A and IV B,

to identify an abnormal region according to conditions (i) or (ii), respectively. We will then combine these into a single $a(\mathbf{r})$ in subsection IV C.

A. Abnormal regions where exchange can dominate: one-electron, rapidly-varying, and nonuniform high-density regions

As discussed earlier, no error cancellation between exchange and correlation can be expected in abnormal regions where the density is too one-electron-like, too rapidly- varying over space, or too high, so there is no reason not to use full exact exchange there. In regions where the density is slowly-varying over space, we might accurately use either full exact exchange ($a = 1$) or semilocal exchange ($a = 0$), but semilocal exchange is computationally preferable because it avoids the need to integrate over the long tail of the exact exchange hole.

Consider the interesting density- and position-dependent variable

$$
u = \frac{\epsilon_{\mathrm{c}}^{\mathrm{GL2TPSS}}}{\epsilon_{\mathrm{x}}^{\mathrm{LSD}}},
\tag{16}
$$

where

$$
\epsilon_{\mathrm{c}}^{\mathrm{GL2TPSS}}([n_\uparrow, n_\downarrow]; \mathbf{r}) = \lim_{\lambda \to \infty} \epsilon_{\mathrm{c}}^{\mathrm{TPSS}}([n_{\uparrow\lambda}, n_{\downarrow\lambda}]; \lambda^{-1}\mathbf{r})
\tag{17}
$$

is the Görling–Levy [68] second-order or high-density limit of the TPSS correlation energy per electron at position $\mathbf{r}$. The latter tends [16, 18, 69] to a negative finite limiting function of $\lambda\mathbf{r}$ as $\lambda \to \infty$ under the uniform density scaling of Eq. (9). The λ^{-1} factor in Eq. (17) then restores the length scale of the original density $n(\mathbf{r})$. An explicit formula for $\epsilon_{\mathrm{c}}^{\mathrm{GL2TPSS}}$ is given in Appendix A. Moreover,

$$
\epsilon_{\mathrm{x}}^{\mathrm{LSD}}([n_\uparrow, n_\downarrow]; \mathbf{r}) = -\frac{3}{4}\left(\frac{3}{\pi}\right)^{1/3} \frac{(2n_\uparrow)^{4/3} + (2n_\downarrow)^{4/3}}{2(n_\uparrow + n_\downarrow)}
\tag{18}
$$

is the LSD exchange energy per electron at $\mathbf{r}$. Note that u vanishes in the one-electron and rapidly-varying limits (because $\epsilon_{\mathrm{c}}^{\mathrm{GL2TPSS}}$ does), and u also vanishes in the high-density limit (because $1/\epsilon_{\mathrm{x}}^{\mathrm{LSD}}$ does).

Now we choose a mixing fraction $a_1(\mathbf{r})$ as a function of u which falls monotonically from 1 at $u = 0$ to 0 as $u \to \infty$. Experience with global hybrid functionals (in which a is independent of $\mathbf{r}$) suggests that a_1 might be a weak function of u over a wide range of u. Thus we try

$$
a_1 = \frac{1}{1 + A\ln(1 + Bu)},
\tag{19}
$$

where A and B are positive empirical parameters. This function is plotted in Fig. 1.

In Eq. (7), the first term on the extreme right is the exact-exchange energy per electron, while the sum of the
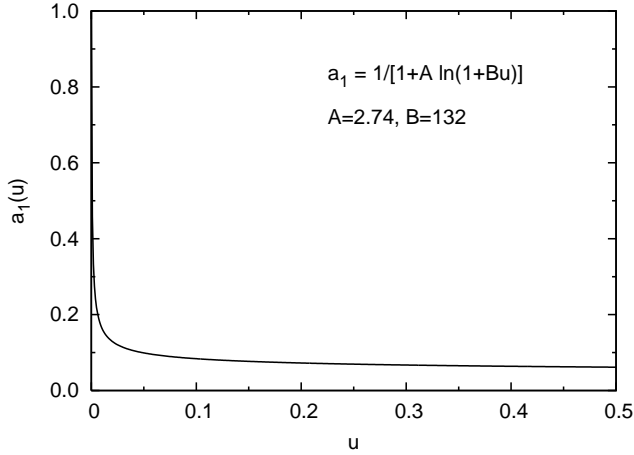
FIG. 1: Mixing fraction $a_1(u)$ of Eq. (19). The values of parameters A and B were fitted as explained in Section V.

middle and last terms is the local hybrid correlation energy per electron ϵ_c^{lh}. We will now verify that many of the exact constraints satisfied by TPSS correlation are also satisfied by our local hybrid correlation.

For a one-electron density, properly $\epsilon_c^{TPSS} = 0$ [18, 69], so $\epsilon_c^{GL2TPSS} = 0$, $u = 0$, and $a_1 = 1$. Thus properly $\epsilon_c^{lh} = 0$. Unlike the semilocal functionals, our local hybrid is exact for all one-electron densities (H, H_2^+, etc.)

In the rapidly-varying limit, in which

$$s = \frac{|\nabla n|}{2(3\pi^2)^{1/3}n^{4/3}} \to \infty, \qquad (20)$$

$\epsilon_c^{TPSS} \to 0$ [16, 18, 69] so $\epsilon_c^{GL2TPSS} \to 0$, $u \to 0$, and $a_1 \to 1$. Thus, $\epsilon_c^{lh} \to 0$. In the exponential tail of an electron density, this is the correct behavior. Under one-dimensional density scaling to the true two-dimensional limit [62, 70, 71], ϵ_c^{lh} is correctly finite, although in this case the limiting function should properly be negative and not zero.

In the nonuniform high-density limit [$\lambda \to \infty$ under the uniform scaling of Eq. (9)], in which $1/\epsilon_x^{LSD} \to 0$, we find $u \to 0$ and $a_1 \to 1 - ABu$. Then

$$\epsilon_c^{lh} \to AB\epsilon_c^{GL2TPSS}\left(\frac{\epsilon_x^{TPSS} - \epsilon_x^{ex}}{\epsilon_x^{LSDA}}\right) + \epsilon_c^{GL2TPSS}. \quad (21)$$

The limit on the right of Eq. (21) is a function of $\lambda\mathbf{r}$, but one that does not otherwise scale with λ. This is properly a finite limit [68] (if not always a properly negative one), implying Eq. (8) and demonstrating that our local hybrid has full exact exchange. The first term on the right of Eq. (21) can be interpreted as the Görling–Levy limit of the static correlation term in our local hybrid correlation of Eq. (7). (Only when the static correlation energy arises from an *exact* degeneracy of the Kohn–Sham noninteracting system can the corresponding limit of the exact static correlation energy not be finite [10].)

There are two regions of an atom or molecule in which $a_1 \to 1$ is expected (and found by our local hybrid):

the rapidly-varying exponential density tail and the high-density region of the deep core. For the rapidly-varying density of a quantum well whose thickness shrinks down to zero (the true two-dimensional limit), $a_1 \to 1$ is also expected (and found); our local hybrid improves greatly but imperfectly [62] upon TPSS and other semilocal functionals in this limit.

In the slowly-varying limit, in which s and other dimensionless density derivatives tend to zero, we have $\epsilon_c^{TPSS} \to \epsilon_c^{LSD}$ [16, 18, 69], $\epsilon_c^{GL2TPSS} \to -\infty$ like $\ln s$ and $u \to \infty$, so $a_1 \to 0$ like $1/\ln(-\ln s)$ and $\epsilon_c^{lh} \to \epsilon_c^{TPSS}$. Since the TPSS correlation energy recovers [16, 18, 69] the second-order gradient expansion [33] in this limit, so does our local hybrid functional.

Finally, we note that in the many-electron low-density limit [$\lambda \to 0$ under the uniform scaling of Eq. (9)], $1/\epsilon_x^{LSD} \to -\infty$, so $u \to \infty$, $a_1 \to 0$, and $\epsilon_{xc}^{lh} \to \epsilon_{xc}^{TPSS}$. There are reasons [72] to believe that TPSS is accurate (although not exact) for the exchange-correlation energy in this limit: As correlation becomes stronger in comparison with exchange, more error cancellation between TPSS exchange and TPSS correlation is expected.

We have not been able to prove, for all possible densities, that the local hybrid correlation energy is always negative or that the Lieb–Oxford bound on its exchange-correlation energy is always satisfied. These constraints are easier to guarantee with semilocal functionals [16, 18, 69] than with local hybrids.

This a_1 makes our exchange-correlation functional exact in the one-electron and high-density limits, and more correct in the rapidly-varying limit. It should provide a $-1/r$ asymptote for the effective exchange-correlation potential around an atom or molecule in the limit $r \to \infty$, needed to bind small negative ions [3] and also needed in time-dependent density functional theory [2] when the electron density is driven far from the nuclei. But it cannot deal with the class of problems addressed in the next section.

B. Abnormal regions where the hole density does not integrate to −1: Open subsystems of fluctuating electron number

Semilocal approximations to the density functional for the exchange-correlation energy assume that the exact exchange-correlation hole density around an electron integrates to −1 on the scale of the local Fermi wavelength, as it does in an electron gas of slowly-varying density. Regions where this is not true, e.g., open subsystems of fluctuating electron number where Δ_{xc} of Eq. (14) is nonzero [5, 10], are therefore abnormal.

Consider the second interesting density- and position-dependent variable

$$v = \frac{\epsilon_x^{ex}}{\epsilon_x^{TPSS}}. \qquad (22)$$

Where v is sufficiently less than 1, we can conclude [by

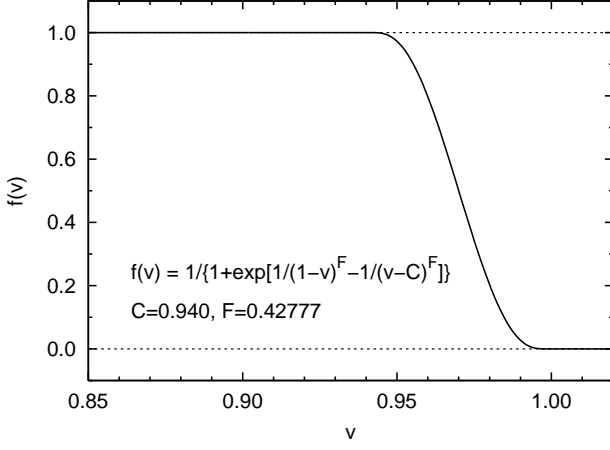FIG. 2: Function $f(v)$ of Eq. (23). The value of C was found as explained in Section V. F is related to C by Eq. (24).

FIG. 3: Function $g(x)$ defined by Eq. (27). The values of parameters D and E were fitted as explained in Section V.

the argument around Eqs. (13) and (14)] that Δ_x of Eq. (5) is positive. Because correlation suppresses density fluctuation [73], we can expect $\Delta_{xc} \leq \Delta_x$. We seek a mixing fraction a_2 such that $a_2 \approx 1$ when $\Delta_{xc} \approx \Delta_x \gg 0$, but $a_2 \approx 0$ when $\Delta_{xc} \approx 0$.

A first candidate for a_2 is

$$
f(v) = \begin{cases} 1, & v \leq C \\ \dfrac{1}{1 + \exp[1/(1-v)^F - 1/(v-C)^F]}, & C < v < 1 \\ 0, & v \geq 1 \end{cases}
\tag{23}
$$

where $C \leq 1$ is an empirical parameter. We have found that we can make $f(v)$ flat around $v = 1$ or C, but not too steep at the midpoint $v = (1+C)/2$, over a wide range of $C < 1$, by choosing

$$
F = -\frac{3}{2\ln[(1-C)/2]} > 0.
\tag{24}
$$

The function $f(v)$ must be flat near $v = 1$ since values of v slightly less than 1 can arise even in normal regions. It interpolates smoothly between 1 (at the highly abnormal $v < C$) and 0 (at the normal $v \approx 1$), reaching $1/2$ at the midpoint $v = (1+C)/2$, as illustrated in Fig. 2. If C is close to 1, there is a sharp step in $f(v)$ which is smoothed when $f(v)$ is multiplied by $\epsilon_x^{\text{TPSS}} - \epsilon_x^{\text{ex}} = (1-v)\epsilon_x^{\text{TPSS}}$. In practical calculations, the function $f(v)$ is best evaluated not by Eq. (23) but as described in Appendix B.

If Δ_{xc} were always equal to Δ_x, we could take $a_2 = f(v)$. But the inequality $\Delta_{xc} \leq \Delta_x$ leads us to consider simple examples in which $v \ll 1$. This situation arises in certain stretched-bond diatomic molecules, with the bond length tending to infinity.

(a) In stretched H_2^+ [74], a single electron is shared equally between two well-separated protons as $H^{+1/2} \cdots H^{+1/2}$. The electron fluctuates between the two proton centers, making $\Delta_{xc} = \Delta_x > 0$ on each center. The Hartree–Fock or exact-exchange-only energy is correctly equal to the sum of the Hartree–Fock energies for
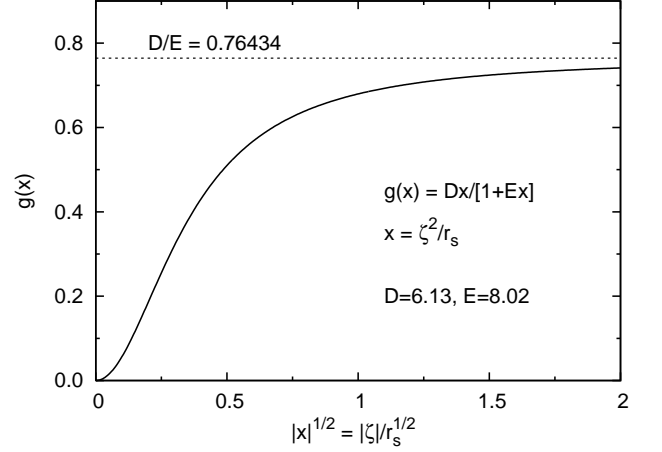
H and H^+, while the TPSS meta-GGA energy is 0.102 hartree (64.0 kcal/mol) too low compared to the sum of the TPSS energies for the integer-charge fragments. In this case, we want full exact exchange or $a_2 = 1$.

(b) In stretched neutral H_2 [10, 24, 25, 75], two electrons are shared equally between two well-separated protons. In the exact singlet ground-state wave function, there is always exactly one electron on each proton center, because of static correlation arising from a Kohn–Sham degeneracy which becomes exact in the limit of infinite bond length, and each H "atom" is spin-unpolarized as a result of fluctuation between "up" and "down" spin, making $\Delta_{xc} = 0$ but $\Delta_x > 0$. The Hartree–Fock or exact-exchange-only energy is incorrectly 0.285 hartree (179 kcal/mol) above the Hartree-Fock energy of two atoms. The corresponding TPSS error is reduced to 0.083 hartree (51.8 kcal/mol). In this case, we want no exact exchange or $a_2 = 0$. We can define an average $\bar{v} = E_x^{\text{ex}}/E_x^{\text{TPSS}}$, where both E_x^{ex} and E_x^{TPSS} are evaluated with the converged TPSS orbitals. For a predominantly normal system, $\bar{v}$ is close to 1 (e.g., 0.97 in H_2^+ and 0.99 in singlet H_2 at the respective equilibrium bond lengths), but $\bar{v}$ is significantly less than 1 in abnormal systems (0.62 in infinitely-stretched H_2^+ and 0.61 in infinitely-stretched singlet H_2).

The hyper-GGA ingredient that seems to distinguish between these two cases is the relative spin polarization

$$
\zeta = \frac{n_\uparrow - n_\downarrow}{n_\uparrow + n_\downarrow},
\tag{25}
$$

which equals ± 1 for stretched H_2^+ and 0 for stretched H_2. Thus we try

$$
a_2 = g\left(\frac{\zeta^2}{r_s}\right) f(v),
\tag{26}
$$

where $n = 3/4\pi r_s^3$ and, setting $x = \zeta^2/r_s$,

$$
g(x) = \frac{Dx}{1 + Ex},
\tag{27}
$$

in which D and E are positive empirical parameters, with $D \leq E$. Eq. (27) is, like the exchange-correlation energy itself, invariant under $\zeta \rightarrow -\zeta$. It interpolates between 0 (at $x = 0$) and D/E (as $x \rightarrow \infty$), as shown in Fig. 3 Our a_2 vanishes when $\zeta \rightarrow 0$ (as in singlet H_2), but also when $r_s \rightarrow \infty$ (i.e., in the low-density limit where correlation can become as strong as exchange, increasing the possibility of error cancellation). With this choice, it may be possible to get an improvement in much of time-independent chemistry and condensed matter physics from a_2 alone, although a_1 is still needed for the situations described at the end of section IV A. The selection of ζ as an ingredient of a_2 is not altogether satisfactory, since it is motivated by simple examples and not by general physical principles.

Our simple examples will now be discussed further: (i) In stretched H_2^+, we have a one-electron density which is already properly described by $a_1 = 1$ from section IV A. (ii) In stretched H_2, the standard spin-symmetry breaking of semilocal functionals, which has a good physical basis [67], will localize a spin-up electron on one proton center, and a spin-down electron on the other, making $|\zeta| = 1$ almost everywhere and eliminating fluctuations (making $\Delta_x = 0$).

Under the uniform density scaling of Eq. (9), $v(\mathbf{r}) \rightarrow v(\lambda \mathbf{r})$ and $\zeta(\mathbf{r}) \rightarrow \zeta(\lambda \mathbf{r})$ and $r_s(\lambda \mathbf{r}) \rightarrow \lambda^{-1} r_s(\mathbf{r})$. [Similarly, for s of Eq. (20), $s(\mathbf{r}) \rightarrow s(\lambda \mathbf{r})$]. In the high-density limit, our a_2 (like our a_1) properly has an expansion in powers of r_s (or λ^{-1}).

We have invoked five empirical parameters: two (A and B) in a_1 and three (C, D, and E) in a_2. Next we will combine our two mixing coefficients into one.

C. Combination rule for the mixing fractions a_1 and a_2

We must combine the mixing fractions a_1 and a_2 from sections IV A and IV B to get a single mixing fraction a for use in Eq. (7), with the following features: (i) $0 \leq a \leq 1$, as expected for any local or global hybrid, (ii) $a = 1$ when *either* $a_1 = 1$ or $a_2 = 1$, because either condition indicates a strongly abnormal region in which full exact exchange can be used. (iii) $a = a_2$ when $a_1 = 0$ and $a = a_1$ when $a_2 = 0$, since in either case all the abnormality of a region is of either one type or the other. Condition (iii) also ensures that $a = 0$ when $a_1 = a_2 = 0$, indicating a strongly normal region in which semilocal approximations suffice. More generally, $a > \max(a_1, a_2)$, because a should increase with abnormality.

A combination rule which satisfies all these expectations is

$$a = 1 - (1 - a_1)(1 - a_2) = a_1 + a_2 - a_1 a_2. \quad (28)$$

Note that, in a nearly-normal region where a_1 and a_2 are small, we find $a \approx a_1 + a_2$. Combining a_1 with a_2 does not lose any of the exact constraints satisfied by a_1 alone. The flatness of $f(v)$ at $v = 1$ preserves the correct
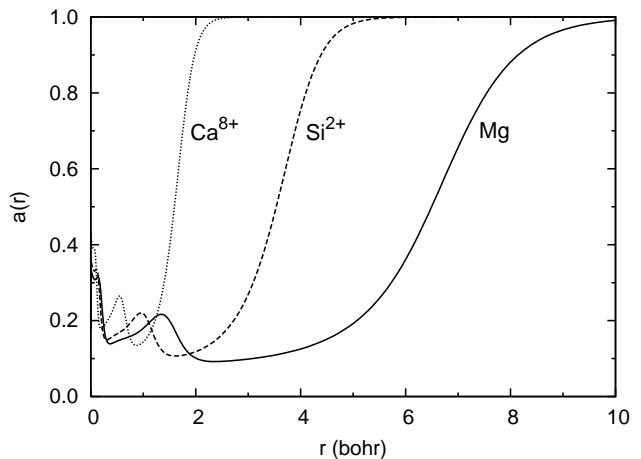

FIG. 4: PSTS hyper-GGA mixing fractions a constructed for the Mg atom and isoelectronic Si^{2+} and Ca^{8+} ions using self-consistent TPSS orbitals obtained in Partridge's uncontracted basis sets [76, 77, 78, 79]: (20s,12p) for Mg; (20s,15p) for Si; (23s,16p) for Ca. The parameters of a are given in Section V. Here $\zeta = 0$, so $a_2 = 0$ and $a = a_1$. The figure illustrates that our mixing fraction a tends smoothly to 1 in the low-density tail, and slowly to 1 in the core in the high-density ($Z \rightarrow \infty$) limit.

gradient expansion for correlation in the slowly-varying limit. The AB term of the high-density ($\lambda \rightarrow \infty$) limit of Eq. (21) is multiplied by the finite $1 - a_2(\lambda \mathbf{r})$, and so remains finite.

For the convenience of having a name, we will call the constructed local hybrid functional the PSTS hyper-GGA. The behavior of the PSTS hyper-GGA mixing fraction a and its components (with parameters fitted as described in Section V) is illustrated by Figs. 4–6. These figures are qualitatively reasonable, as discussed near the end of section VI.

V. FITTING THE PARAMETERS TO STANDARD ENTHALPIES OF FORMATION AND BARRIER HEIGHTS

We have determined the five empirical parameters (A, B, D, C, E) of the PSTS hyper-GGA mixing fraction $a(\mathbf{r})$ by minimizing the quantity

$$S_W = \frac{1}{2} \left[\text{MAE(G2/97)} + \text{MAE(BH42/03)} \right], \quad (29)$$

where MAE(G2/97) is the calculated mean absolute error of 148 standard enthalpies of formation of the molecules of the G2/97 test set [48], and MAE(BH42/03) is the mean absolute error of 42 forward and reverse barrier heights of the 21 gas-phase hydrogen-transfer reactions of the BH42/03 test set [49]. The molecules of the G2/97 set are built up from hydrogen and/or first- and second-row atoms, and all but one of the reactions of the BH42/03
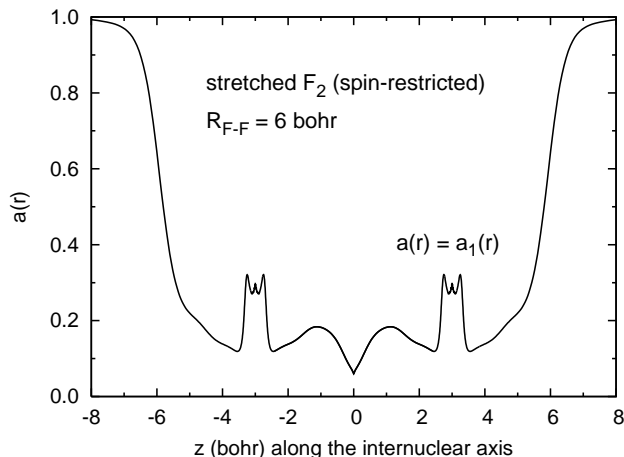
FIG. 5: PSTS hyper-GGA mixing fraction a constructed with self-consistent TPSS/u-6-311++G(3df,3pd) orbitals along the internuclear axis of a stretched F_2 molecule ($z = 0$ is the center of the bond). In all regions shown, $a_2 = 0$ and $a = a_1$. The parameters of a are given in Section V. Note that a has a cusp at $z = 0$ which seems unphysical but is limited to a very small region of three-dimensional space.
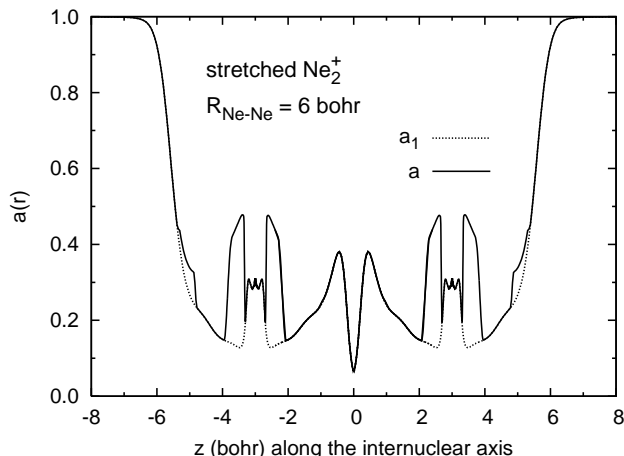

FIG. 6: PSTS hyper-GGA mixing fractions a_1 and a constructed with self-consistent TPSS/u-6-311++G(3df,3pd) orbitals along the internuclear axis of a stretched Ne_2^+ molecular ion ($z = 0$ is the center of the bond). The parameters of a are given in Section V. In some regions, $a_2 > 0$ and $a > a_1$.

test set involve atomic and molecular radicals (i.e., spin-unpaired systems) as reactants. The reference values of the standard enthalpies of formation are all experimental, while the 42 barriers are best estimates based on a combination of experimental reaction rates and high-level electronic structure calculations [49]. The mean signed error of standard enthalpies of formation is roughly equal and opposite to the mean signed error of the corresponding atomization energies, whereas the mean absolute errors are about the same. The rather complicated methodology of evaluating the standard enthalpies of formation is

documented in Ref. 19. The only difference between the present procedure and the one of Ref. 19 is that here we employed the fully uncontracted 6-311++G(3df,3pd) basis set for calculating the electronic energies rather than the standard (contracted) 6-311++G(3df,3pd) basis [78], because the latter is not well-suited for the resolution of the identity used for evaluating $\epsilon_x^{ex(conv)}$ and ϵ_x^{ex} [57].

We do not have yet a fully self-consistent implementation of our local hybrid functional and so evaluate all hyper-GGA energies using converged TPSS orbitals. We speculate, based on our studies of a previous version of the hyper-GGA, that the choice of orbitals would have a small effect on the results for enthalpies of formation and barrier heights, provided that the parameters of the functional are optimized for each choice.

The optimized values of the hyper-GGA parameters obtained in this manner are as follows: $A = 2.74$, $B = 132$, $C = 0.940$, $D = 6.13$, and $E = 8.02$. Although the G2/97 and BH42/03 training sets differ markedly in size, their equal weighting in Eq. (29) does not cause a significant bias in favor of the data included in either test set because both sets are sufficiently representative of the types of molecules/reactions they contain.

In Table I, we compare the performance of our PSTS hyper-GGA with that of simpler functionals constructed by the method of constraint satisfaction with no or minimal empiricism. The functionals not already introduced in Section I are: HFx/TPSSc is the Hartree–Fock exchange with TPSS correlation, PBEh is the global hybrid PBE functional with $a = 0.25$ [46, 81, 82], and TPSSh is the global TPSS hybrid with $a = 0.10$ [19]. Among the approximations included in Table I, the PSTS hyper-GGA is overall the most accurate (has the smallest S_W). To put these results into perspective, we point out that the mean experimental atomization energy for the G2/97 set of molecules is 478.5 kcal/mol, while the mean experimental barrier height for the BH42 set of reaction barriers is 14.0 kcal/mol. Note that although the PSTS hyper-GGA has been trained on G2/97, it has an even better performance for the larger G3/99 test set [44] of 223 molecules (including COF_2), for which the mean experimental atomization energy is $\sim$1180 kcal/mol.

Table I also shows results for two simplified hyper-GGAs labeled "hyper-GGA (conv.)" and "hyper-GGA ($a = a_1$)". The former differs from the PSTS hyper-GGA in that it uses the conventional exact-exchange energy per electron $\epsilon_x^{ex(conv)}$ in place of the gauge-transformed ϵ_x^{ex} of Eq. (12). The five empirical parameters of this form, determined by minimizing S_W, are as follows: $A = 3.14$, $B = 146$, $C = 0.930$, $D = 5.17$, and $E = 9.49$. This form performs slightly worse than the PSTS hyper-GGA, which is consistent with our argument that local hybrids should combine exact and semi-local exchange in the same gauge. The second simplified hyper-GGA uses ϵ_x^{ex} in the TPSS gauge but has a_2 set to zero, so its mixing fraction $a = a_1$ depends only on parameters A and B (whose optimized values are $A = 2.77$ and $B = 545$). Because this a is close to 0.1 for nearly all relevant val-

TABLE I: Relative performance of the PSTS and two simplified hyper-GGAs for the G2/97 and G3/99 test sets of standard enthalpies of formation (148 and 223 molecules, respectively) and the BH42/03 set of 42 reaction barriers. The test sets are described in Section V. G2/97 is a subset of G3/99. ME is the mean error (signed) relative to reference values, MAE is the mean absolute error. S_W is defined by Eq. (29). All calculations were carried out with a development version of the GAUSSIAN program [80] using the fully uncontracted 6-311++G(3df,3pd) basis set. All values are in kcal/mol. For comparison, the mean atomization energies are 478.5 kcal/mol for G2/97 and 1180 kcal/mol for G3/99, while the mean reaction barrier height is 14.0 kcal/mol (BH42/03). 1 kcal/mol $\approx$ 0.0434 eV $\approx$ 0.00159 hartree.

Method	G2/97		BH42/03			G3/99			
	ME	MAE	ME	MAE	S_W	ME	MAE	Max. (+)	Min. (−)
Hartree–Fock	148.0	148.0	12.5	12.8	80.4	211.0	211.0	581.0 (C_8H_{18})	−0.6 (BeH)
HFx/TPSSc	25.2	27.7	4.2	5.8	16.7	27.7	30.3	130.0 (O_3)	−23.1 (Si_2H_6)
LSDA[a]	−83.4	83.4	−18.1	18.1	50.7	−121.2	121.2	0.6 (Li_2)	−344.3 ($C_{10}H_8$)
PBE GGA	−16.1	16.9	−9.7	9.7	13.3	−21.6	22.1	10.8 (Si_2H_6)	−78.9 ($C_{10}H_8$)
TPSS meta-GGA	−5.7	6.4	−8.4	8.4	7.4	−6.0	6.5	15.0 (SiF_4)	−23.9 (ClF_3)
PBEh	−2.6	5.0	−4.7	4.7	4.8	−5.0	6.8	20.5 (SiF_4)	−35.8 ($C_{10}H_8$)
TPSSh	−1.9	4.4	−6.6	6.6	5.5	−1.6	4.1	20.8 (SiF_4)	−18.0 (Si_2H_6)
PSTS hyper-GGA[b]	−0.6	4.7	−1.2	2.1	3.4	−0.2	4.5	23.2 (SiF_4)	−19.1 (Si_2H_6)
Hyper-GGA (conv.)[b]	−0.8	5.6	−1.2	2.3	3.9	−0.2	5.5	28.7 (SiF_4)	−21.5 (Si_2H_6)
Hyper-GGA ($a = a_1$)[b]	0.2	4.5	−6.6	6.6	5.5	1.5	4.7	26.5 (SiF_4)	−19.0 (Si_2H_6)

[a] Using the Perdew–Wang representation [15] of $\epsilon_c^{LSDA}(r_s, \zeta)$.

[b] All hyper-GGA energies were evaluated using self-consistent TPSS orbitals.

ues of $u(\mathbf{r})$, the performance of the a_1-only hyper-GGA is very similar to that of TPSSh (a global hybrid with $a = \text{const} = 0.1$): atomization energies are more accurate than from the TPSS meta-GGA, but there is little improvement for reaction barriers.

VI. CONCLUSIONS

We have argued that semilocal density functionals work in many cases because of a justified cancellation of errors between exchange and correlation that occurs in identifiable "normal" regions. This enables one to construct nonempirical semilocal functionals (such as LSD, PBE GGA, and TPSS meta-GGA) on the first three rungs of a ladder of increasingly sophisticated approximations. The fourth or hyper-GGA rung requires empirical parameters to balance the full nonlocality of correlation against that of exact exchange, since known exact constraints say nothing about this balance. (At least this is so when we consider only exact constraints on the integrated exchange-correlation energy; a correlation factor [83], applied to a nearly-exact exchange hole density of an inhomogeneous system [84], might work or might not without empiricism). Our PSTS hyper-GGA is a local hybrid, mixing in a fraction a of exact exchange locally, according to Eqs. (7), (19), (26), and (28). Because our a tends to one in the high-density limit, our hyper-GGA has full exact exchange. It is also one-electron self-interaction-free and size-consistent.

The small relative error (typically of order 1% or less) of the TPSS meta-GGA for the atomization energies of molecules suggests that these quantities are dominated by contributions from normal regions. The much larger

relative error (typically of order 60%) of the TPSS meta-GGA for the barrier heights to chemical reactions suggests that those quantities contain substantial contributions from abnormal regions. Thus we fit our hyper-GGA parameters simultaneously to atomization energies (preserving and slightly improving them, mainly via our local mixing fraction a_1) and to barrier heights (substantially improving them, mainly through our local mixing fraction a_2).

We have invoked five empirical parameters (A, B, C, D, E), probably close to the minimum possible number since there are four kinds of abnormal regions. But, as more empirical parameters are introduced, there is a graver danger of "overfitting" any given limited data set. A fit that is unjustifiably good can worsen results for systems and properties very different from those that have been fitted. We have tried to minimize this danger by fitting to forms which take into account known exact constraints, physical insights, and paradigm examples.

To construct our PSTS hyper-GGA, we satisfy exact constraints on the density functional for the exchange-correlation energy. Of all the constraints possible for a hyper-GGA, the only one we have not tried to satisfy is the non-zero limit [69] for the correlation energy under one-dimensional density scaling to the true two-dimensional limit. In this limit, our PSTS hyper-GGA correlation energy tends to zero (as in the TPSS meta-GGA); the correct non-zero limit seems too complicated to incorporate in any simple way, and not very relevant to most physical systems. Moreover, two exact constraints that are guaranteed for all possible densities at the TPSS meta-GGA level are no longer so guaranteed in local hybrids like PSTS: the non-positivity of the correlation energy and the Lieb–Oxford lower bound on

the exchange-correlation energy. Of course, the PSTS exchange-correlation energy is negative for all possible densities.

Apart from the need for empirical parameters, constraint satisfaction is the same method used earlier to construct the PBE GGA [16] and the TPSS meta-GGA [18]. In the hyper-GGA case, we satisfy additional exact constraints via a careful interpolation between a semilocal exchange energy density in a normal region and the exact exchange energy density in an abnormal region. Our method combines (and goes beyond) some of the best formal features of other methods, including the size-consistency of methods that model the exchange-correlation hole density [24, 25, 35, 43] and the proper concern for the high-density (or weakly-interacting) and low-density (or strongly-interacting) limits of methods that model the integrand $W_\alpha[n]$ of the coupling-constant integral [26, 27, 45, 46, 58]

$$E_{\text{xc}}[n] = \int_0^1 d\alpha \, W_\alpha[n]. \tag{30}$$

Of course, our PSTS hyper-GGA has its own hole model [namely, Eq. (15)] and its own coupling-constant integrand [68, 85] defined by

$$W_\alpha[n] = \frac{d}{d\alpha}(\alpha^2 E_{\text{xc}}[n_{1/\alpha}]). \tag{31}$$

The behavior of our abnormality index or local exact-exchange mixing fraction $a(\mathbf{r})$, as illustrated in Figs. 4–6, is qualitatively reasonable: For an isolated many-electron atom of fixed electron number (Fig. 4) it is small (≈ 0.1) in the valence region but larger (≈ 0.3) in the higher-density core, and it gradually approaches 1 in the rapidly-varying exponential tail. For a stretched molecule, it is atomic-like around an atom of weakly-fluctuating electron number (Fig. 5 for spin-restricted stretched F_2), but much larger (≈ 0.4) in the relevant valence region of an atom of strongly-fluctuating electron number (Fig. 6 for stretched Ne_2^+). A version of the last effect is what raises and improves the barrier heights in Table I.

Figure 4 shows a slow increase of a in the core as the atomic number Z increases from 12 (Mg) to 14 (Si^{2+}) to 20 (Ca^{8+}). At large Z, there is a uniform density scaling to the high-density limit in the core, so that $a \to 1$ as $Z \to \infty$. The slowness of the approach to 1 is not a problem, since TPSS meta-GGA (unlike LSDA) exchange is accurate for localized core-electron densities.

Figure 5 shows a seemingly unphysical cusp in a at the bond center, where for the symmetric stretched molecule F_2 the reduced density gradient $s \to 0$ and thus our $a \to 0$ (although the approach to 0 cannot be plotted on the scale of this figure). This cusp is a consequence of our Eqs. (16) and (19), since $u \to \infty$ as $s \to 0$. By recovering semilocality in the limit of slowly-varying density, we have introduced an artifact in a small volume around the bond center. Stretched Ne_2^+ in Fig. 6 also displays a bond-center cusp. Even the TPSS meta-GGA exchange

by itself can have a bond-center artifact [72]. So far as we know, these artifacts are harmless.

The ideas in this paper are general ones that may be generally useful. On the other hand, our way of implementing them is far from unique. In future work, we hope to continue to refine and test this approach to the hyper-GGA including its self-consistent implementation.

APPENDIX A: EXPRESSION FOR $\epsilon_{\text{c}}^{\text{GL2TPSS}}$

The Görling–Levy second-order limit of the TPSS correlation energy per electron $\epsilon_{\text{c}}^{\text{GL2TPSS}}$ is given by

$$\epsilon_{\text{c}}^{\text{GL2TPSS}} = \epsilon_{\text{c}}^{\text{GL2revPKZB}}\left[1 + d\epsilon_{\text{c}}^{\text{GL2revPKZB}}\left(\frac{\tau_W}{\tau}\right)^3\right], \tag{A1}$$

where $d = 2.8$ hartree^{-1} is a constant and

$$\begin{aligned}\epsilon_{\text{c}}^{\text{GL2revPKZB}} &= \epsilon_{\text{c}}^{\text{GL2PBE}}(n_\uparrow, n_\downarrow, \nabla n_\uparrow, \nabla n_\downarrow)\left[1 + C(\zeta, \xi)\left(\frac{\tau_W}{\tau}\right)^2\right] \\ &\quad - [1 + C(\zeta, \xi)]\left(\frac{\tau_W}{\tau}\right)^2 \sum_\sigma \frac{n_\sigma}{n}\tilde{\epsilon}_{\text{c},\sigma}^{\text{GL2PBE}}. \end{aligned} \tag{A2}$$

In Eq. (A2), $\epsilon_{\text{c}}^{\text{GL2PBE}}$ is the Görling–Levy limit of the PBE correlation energy per electron. It is obtained by replacing $\lambda\mathbf{r}$ with $\mathbf{r}$ in the $\lambda \to \infty$ uniform density scaling limit of the PBE correlation energy per electron [16]:

$$\begin{aligned}\epsilon_{\text{c}}^{\text{GL2PBE}}&(n_\uparrow, n_\downarrow, \nabla n_\uparrow, \nabla n_\downarrow) \\ &= -\gamma\phi^3 \ln\left[1 + \frac{1}{\chi s^2/\phi^2 + (\chi s^2/\phi^2)^2}\right], \end{aligned} \tag{A3}$$

in which $\gamma = (1 - \ln 2)/\pi^2$,

$$\phi(\zeta) = \frac{1}{2}\left[(1 + \zeta)^{2/3} + (1 - \zeta)^{2/3}\right], \tag{A4}$$

$s = |\nabla n|/2nk_F$ is the reduced density gradient of Eq. (20), $k_F = (3\pi^2 n)^{1/3}$, and $\chi = (\beta/\gamma)c^2 e^{-\omega/\gamma} \approx 0.72161$, where $c = (3\pi^2/16)^{1/3}$, $\beta = 0.066725$, and $\omega = 0.046644$ [16]. The spin-dependent function $\tilde{\epsilon}_{\text{c},\sigma}^{\text{GL2PBE}}$ is defined [18, 72] as

$$\begin{aligned}\tilde{\epsilon}_{\text{c},\sigma}^{\text{GL2PBE}} = \max\big[&\epsilon_{\text{c}}^{\text{GL2PBE}}(n_\sigma, 0, \nabla n_\sigma, 0), \\ &\epsilon_{\text{c}}^{\text{GL2PBE}}(n_\uparrow, n_\downarrow, \nabla n_\uparrow, \nabla n_\downarrow)\big]. \end{aligned} \tag{A5}$$

The function $C(\zeta, \xi)$, where ζ is the spin-polarization of Eq. (25) and $\xi = |\nabla\zeta|/2k_F$, is given by Eq. (14) of Ref. 18.

APPENDIX B: EVALUATION OF $f(v)$

The exponent $1/(1 - v)^F - 1/(v - C)^F$ appearing in Eq. (23) tends to $+\infty$ as v approaches 1 from below. In order to avoid numerical overflow problems with the

exponential term of $f(v)$ in the interval $C < v < 1$, Eq. (23) may be rewritten as follows. Define

$$p_1 = \frac{1}{(1-v)^F}, \quad p_C = \frac{1}{(v-C)^F}. \qquad \text{(B1)}$$

Then, inside the interval $C < v < 1$,

$$f(v) = \begin{cases} \dfrac{1}{1 + e^{p_1 - p_C}}, & \text{if } p_1 \le p_C \\[2ex] \dfrac{e^{p_C - p_1}}{1 + e^{p_C - p_1}}, & \text{if } p_C \le p_1 \end{cases} , \qquad \text{(B2)}$$

which is robust because all exponents are non-positive.

[1] W. Kohn and L. J. Sham, Phys. Rev. **140**, A1133 (1965).

[2] C. Fiolhais, F. Nogueira, and M. Marques, eds., *A Primer in Density Functional Theory* (Springer, Berlin, 2003).

[3] J. P. Perdew and A. Zunger, Phys. Rev. B **23**, 5048 (1981).

[4] J. P. Perdew, R. G. Parr, M. Levy, and J. L. Balduz, Jr., Phys. Rev. Lett. **49**, 1691 (1982).

[5] J. P. Perdew, in *Density Functional Methods in Physics*, edited by R. M. Dreizler and J. da Providência (Plenum, New York, 1985).

[6] A. Ruzsinszky, J. P. Perdew, G. I. Csonka, O. A. Vydrov, and G. E. Scuseria, J. Chem. Phys. **125**, 194112 (2006).

[7] A. Ruzsinszky, J. P. Perdew, G. I. Csonka, O. A. Vydrov, and G. E. Scuseria, J. Chem. Phys. **126**, 104102 (2007).

[8] P. Mori-Sánchez, A. J. Cohen, and W. Yang, J. Chem. Phys. **125**, 201102 (2006).

[9] O. A. Vydrov, G. E. Scuseria, and J. P. Perdew, J. Chem. Phys. **126**, 154109 (2007).

[10] J. P. Perdew, A. Ruzsinszky, G. I. Csonka, O. A. Vydrov, G. E. Scuseria, V. N. Staroverov, and J. Tao, Phys. Rev. A **76**, 040501(R) (2007).

[11] A. Ruzsinszky, J. P. Perdew, G. I. Csonka, G. E. Scuseria, and O. A. Vydrov, Phys. Rev. A **77**, 060502(R) (2008).

[12] J. P. Perdew and K. Schmidt, in *Density Functional Theory and Its Application to Materials*, edited by V. Van Doren, C. Van Alsenoy, and P. Geerlings (AIP, Melville, NY, 2001).

[13] J. P. Perdew, A. Ruzsinszky, J. Tao, V. N. Staroverov, G. E. Scuseria, and G. I. Csonka, J. Chem. Phys. **123**, 062201 (2005).

[14] S. H. Vosko, L. Wilk, and M. Nusair, Can. J. Phys. **58**, 1200 (1980).

[15] J. P. Perdew and Y. Wang, Phys. Rev. B **45**, 13244 (1992).

[16] J. P. Perdew, K. Burke, and M. Ernzerhof, Phys. Rev. Lett. **77**, 3865 (1996); **78**, 1396(E) (1997).

[17] J. P. Perdew, A. Ruzsinszky, G. I. Csonka, O. A. Vydrov, G. E. Scuseria, L. A. Constantin, X. Zhou, and K. Burke, Phys. Rev. Lett. **100**, 136406 (2008).

[18] J. Tao, J. P. Perdew, V. N. Staroverov, and G. E. Scuseria, Phys. Rev. Lett. **91**, 146401 (2003).

[19] V. N. Staroverov, G. E. Scuseria, J. Tao, and J. P. Perdew, J. Chem. Phys. **119**, 12129 (2003); **121**, 11507(E) (2004).

[20] V. N. Staroverov, G. E. Scuseria, J. Tao, and J. P. Perdew, Phys. Rev. B **69**, 075102 (2004).

[21] J. P. Perdew and L. A. Constantin, Phys. Rev. B **75**, 155109 (2007).

[22] F. G. Cruz, K.-C. Lam, and K. Burke, J. Phys. Chem. A **102**, 4911 (1998).

[23] J. Jaramillo, G. E. Scuseria, and M. Ernzerhof, J. Chem. Phys. **118**, 1068 (2003).

[24] A. D. Becke, J. Chem. Phys. **122**, 064101 (2005).

[25] A. D. Becke and E. R. Johnson, J. Chem. Phys. **127**, 124108 (2007).

[26] P. Mori-Sánchez, A. J. Cohen, and W. Yang, J. Chem. Phys. **124**, 091102 (2006).

[27] A. J. Cohen, P. Mori-Sánchez, and W. Yang, J. Chem. Phys. **127**, 034101 (2007).

[28] A. V. Arbuznikov, M. Kaupp, and H. Bahmann, J. Chem. Phys. **124**, 204102 (2006).

[29] M. Kaupp, H. Bahmann, and A. V. Arbuznikov, J. Chem. Phys. **127**, 194102 (2007).

[30] A. V. Arbuznikov and M. Kaupp, J. Chem. Phys. **128**, 214107 (2008).

[31] L. A. Constantin, J. M. Pitarke, J. F. Dobson, A. Garcia-Lekue, and J. P. Perdew, Phys. Rev. Lett. **100**, 036401 (2008).

[32] P. R. Antoniewicz and L. Kleinman, Phys. Rev. B **31**, 6779 (1985).

[33] S.-K. Ma and K. A. Brueckner, Phys. Rev. **165**, 18 (1968).

[34] D. C. Langreth and J. P. Perdew, Phys. Rev. B **21**, 5469 (1980).

[35] A. D. Becke and M. R. Roussel, Phys. Rev. A **39**, 3761 (1989).

[36] P. S. Svendsen and U. von Barth, Phys. Rev. B **54**, 17402 (1996).

[37] A. D. Becke, J. Chem. Phys. **109**, 2092 (1998).

[38] T. Leininger, H. Stoll, H.-J. Werner, and A. Savin, Chem. Phys. Lett. **275**, 151 (1997).

[39] O. A. Vydrov and G. E. Scuseria, J. Chem. Phys. **125**, 234109 (2006).

[40] M. Dion, H. Rydberg, E. Schröder, D. C. Langreth, and B. I. Lundqvist, Phys. Rev. Lett. **92**, 246401 (2004).

[41] S. Kurth, J. P. Perdew, and P. Blaha, Int. J. Quantum Chem. **75**, 889 (1999).

[42] G. I. Csonka, O. A. Vydrov, G. E. Scuseria, A. Ruzsinszky, and J. P. Perdew, J. Chem. Phys. **126**, 244107 (2007).

[43] J. P. Perdew, K. Burke, and Y. Wang, Phys. Rev. B **54**, 16533 (1996); **57**, 14999(E) (1998).

[44] L. A. Curtiss, K. Raghavachari, P. C. Redfern, and J. A. Pople, J. Chem. Phys. **112**, 7374 (2000).

[45] A. D. Becke, J. Chem. Phys. **98**, 5648 (1993).

[46] J. P. Perdew, M. Ernzerhof, and K. Burke, J. Chem. Phys. **105**, 9982 (1996).

[47] Y. Zhao, N. E. Schultz, and D. G. Truhlar, J. Chem. Theory Comput. **2**, 364 (2006).

[48] L. A. Curtiss, K. Raghavachari, P. C. Redfern, and J. A. Pople, J. Chem. Phys. **106**, 1063 (1997).

[49] Y. Zhao, B. J. Lynch, and D. G. Truhlar, J. Phys. Chem. A **108**, 2715 (2004).

[50] F. Furche and J. P. Perdew, J. Chem. Phys. **124**, 044103 (2006).

[51] J. Heyd, G. E. Scuseria, and M. Ernzerhof, J. Chem. Phys. **118**, 8207 (2003).

[52] J. Heyd and G. E. Scuseria, J. Chem. Phys. **121**, 1187 (2004).

[53] J. Paier, M. Marsman, K. Hummer, G. Kresse, I. C. Gerber, and J. G. Ángyán, J. Chem. Phys. **124**, 154709 (2006).

[54] M. Levy, Phys. Rev. A **43**, 4637 (1991).

[55] A. J. Cohen, P. Mori-Sánchez, and W. Yang, J. Chem. Phys. **126**, 191109 (2007).

[56] N. C. Handy and A. J. Cohen, Mol. Phys. **99**, 403 (2001).

[57] J. Tao, V. N. Staroverov, G. E. Scuseria, and J. P. Perdew, Phys. Rev. A **77**, 012509 (2008).

[58] M. Seidl, J. P. Perdew, and S. Kurth, Phys. Rev. Lett. **84**, 5070 (2000).

[59] D. C. Langreth and J. P. Perdew, Solid State Commun. **17**, 1425 (1975).

[60] L. C. Wilson and M. Levy, Phys. Rev. B **41**, 12930 (1990).

[61] Y. Zhao and D. G. Truhlar, J. Phys. Chem. A **110**, 13126 (2006).

[62] L. A. Constantin, J. P. Perdew, and J. M. Pitarke, Phys. Rev. Lett. **101**, 016406 (2008). Note that an earlier version of our PSTS hyper-GGA was tested in this paper; an erratum will update the figure.

[63] O. Gunnarsson and B. I. Lundqvist, Phys. Rev. B **13**, 4274 (1976).

[64] M. Ernzerhof and J. P. Perdew, J. Chem. Phys. **109**, 3313 (1998).

[65] L. A. Constantin, J. P. Perdew, and J. Tao, Phys. Rev. B **73**, 205104 (2006).

[66] K. Burke, J. P. Perdew, and M. Ernzerhof, J. Chem. Phys. **109**, 3760 (1998).

[67] J. P. Perdew, A. Savin, and K. Burke, Phys. Rev. A **51**, 4531 (1995).

[68] A. Görling and M. Levy, Phys. Rev. B **47**, 13105 (1993).

[69] J. P. Perdew, S. Kurth, A. Zupan, and P. Blaha, Phys. Rev. Lett. **82**, 2544 (1999); **82**, 5179(E) (1999).

[70] L. Pollack and J. P. Perdew, J. Phys.: Condens. Matter **12**, 1239 (2000).

[71] A. Görling and M. Levy, Phys. Rev. A **45**, 1509 (1992).

[72] J. P. Perdew, J. Tao, V. N. Staroverov, and G. E. Scuseria, J. Chem. Phys. **120**, 6898 (2004).

[73] P. Ziesche, J. Tao, M. Seidl, and J. P. Perdew, Int. J. Quantum Chem. **77**, 819 (2000).

[74] J. P. Perdew and M. Ernzerhof, in *Electronic Density Functional Theory: Recent Progress and New Directions*, edited by J. F. Dobson, G. Vignale, and M. P. Das (Plenum Press, New York, 1998).

[75] I. N. Levine, *Quantum Chemistry* (Prentice Hall, Englewood Cliffs, 1991), 4th ed., p. 390.

[76] H. Partridge, J. Chem. Phys. **87**, 6643 (1987).

[77] H. Partridge, J. Chem. Phys. **90**, 1043 (1989).

[78] K. L. Schuchardt, B. T. Didier, T. Elsethagen, L. Sun, V. Gurumoorthi, J. Chase, J. Li, and T. L. Windus, J. Chem. Inf. Model. **47**, 1045 (2007).

[79] D. Feller, J. Comput. Chem. **17**, 1571 (1996).

[80] M. J. Frisch, G. W. Trucks, H. B. Schlegel *et al.*, GAUSSIAN Development Version, Revision F.02, Gaussian, Inc., Wallingford, CT, 2006.

[81] M. Ernzerhof and G. E. Scuseria, J. Chem. Phys. **110**, 5029 (1999).

[82] C. Adamo and V. Barone, J. Chem. Phys. **110**, 6158 (1999).

[83] P. Gori-Giorgi and J. P. Perdew, Phys. Rev. B **66**, 165118 (2002).

[84] M. Ernzerhof and H. Bahmann, talk at ISTCP-VI, Vancouver, British Columbia, July 2008.

[85] M. Levy and J. P. Perdew, Phys. Rev. A **32**, 2010 (1985).